Gap anisotropy in high-T_c superconductors: A unified picture

J. R. Kirtley
IBM Thomas J. Watson Research Center, P.O. Box 218, Yorktown Heights, New York 10598
(Received 26 October 1989)

I propose a synthesis of the results of several different gap-measurements techniques by means of a phenomenological, anisotropic model for the energy gap. This model, which has a large gap in the *a-b* plane crystalline direction, and a smaller BCS-sized gap in the *c*-axis direction, is chosen to be consistent with recent infrared, Raman, photoemission, and high-resolution electron-energy-loss data. I show in this paper that it is also consistent with point-contact tunneling data.

Knowledge of the superconducting density of states in the layered copper oxide ceramics is of primary importance for understanding the mechanism for high-T_c superconductivity. Unfortunately, no consensus has been reached on the interpretation of various gap-measurement techniques. There is now a growing body of evidence that the superconducting energy gap in the ceramic high-T_c superconductors is significantly larger than the BCS value in the *a-b* plane. Infrared data on $YBa_2Cu_3O_7$,[1] Raman-scattering experiments on $YBa_2Cu_3O_7$ (Ref. 2) and BiCaSrCuO,[3] photoemission experiments on BiCaSrCuO,[4] and high-resolution electron-energy-loss spectra of $YBa_2Cu_3O_7$ and BiCaSrCuO (Ref. 5) all show structure which develops with the onset of superconductivity and has an energy scale of order $2\Delta\sim(7-8)kT_c$. The tunneling evidence also points towards an energy gap that is significantly larger than the BCS value, but the body of evidence points towards a gap size of order $2\Delta\sim(4-6)kT_c$,[6,7] somewhat smaller than the values inferred from the other measurements. There is also now evidence for gap anisotropy in the high-T_c ceramic superconductors. Infrared measurements[1] and Raman-scattering measurements[2] both indicate substantial anisotropy in the gap in $YBa_2Cu_3O_7$. Because of the difficulties in making junctions smooth on a scale comparable to the short coherence lengths in the high-T_c superconductors, it is likely that most tunneling measurements have been averaged over crystalline orientations. However, there has been a claim of tunneling measurement of anisotropy of the gap in $YBa_2Cu_3O_7$, with a BCS-like dependence of the gap size on critical temperature for tunneling parallel to the *c* axis, and a stronger dependence, about $2\Delta=6kT_c$, for tunneling perpendicular to the *c* axis.[8] I will argue in this paper that the apparent discrepancy between the tunneling and other gap-measurement techniques is due to different samplings of the anisotropic gap, and provide a detailed analysis of the point-contact tunneling data to support this argument, using conventional tunneling theory, and properly accounting for the effects of (i) low tunneling barrier heights, (ii) large superconducting energy gaps, and (iii) gap anisotropy. Explanations for the large conductance backgrounds, smeared gap-edge structures, and "double-humped" structures that are often observed in the tunneling data arise quite naturally from this model.

The large conductance background for voltages above the gap often seen in tunneling measurements of the high-T_c superconductors has been attributed to several mechanisms in the literature, including charging of electrically isolated metallic inclusions in the surface of the superconductor,[9] resonating-valence-bond effects,[10] or a frequency-dependent absorptive part to the polarizability of the superconductor.[11] I will instead take the view in this paper that this conductance background is due to a low effective tunneling barrier in the point-contact junctions. This assumption does not affect the synthesis of results from different gap-measurement techniques which is the central thrust of this paper. However, it provides a straightforward means for fitting the experimental data, and gives a natural explanation for the asymmetry in the amplitudes of the conductance overshoots with voltage often observed. This physical interpretation is in keeping with past tunneling experience, where linear dependences of the conductance background have been frequently observed, for example, in Al-Al_2O_3-Pb junctions with hydrocarbon impurities intentionally introduced at the oxide-Pb interface,[12] and in GaAs-$Al_xGa_{1-x}As$-GaAs heterojunction tunnel junctions.[13]

An expression for the specular tunneling current between a normal metal and a superconductor which is sufficiently general for the purposes of this paper is[14,15]

$$J=\frac{q}{2\pi^2\hbar}\int_0^{E_m}dE_z D(E_z)\int_{-\infty}^{\infty}dk_x\int_{-\infty}^{\infty}dk_y[f(E-qv)-f(E)]\rho_s(E,\hat{\mathbf{k}}), \tag{1}$$

where J is the tunneling current density per unit area, q is the charge on the tunneling carriers, $\hbar$ is Planck's constant, $D(E_z)$ is the barrier penetration probability, $f(E)$ is the Fermi function $f(E)=\{1+\exp[(E-E_f)/kT]\}^{-1}$, E_f is the Fermi energy, k is Boltzmann's constant, T is the temperature, V is the bias voltage, $\rho_s(E,\hat{\mathbf{k}})$ is the effective tunneling density of states of the superconductor, $\hat{\mathbf{k}}$ is the unit vector in the tunneling direction, and the integrations are over wave vectors of the electrons parallel (k_x,k_y) and energies perpendicular (E_z) to the tunneling barrier. The tunneling carrier charge q is taken to be $-e$ for electron tunneling, and $+e$ for hole tunneling, where e is the abso-

lute value of the charge on an electron. The total kinetic energy of the carriers is $E = E_z + E_\parallel$. In the parabolic band approximation $E_\parallel = \hbar^2(k_x^2/2m_x + k_y^2/2m_y)$, where $m_{x,y}$ are the effective masses of the carriers in the plane parallel to the tunneling barrier. In the Wentzel-Kramers-Brillouin approximation the barrier penetration probability is given by[14]

$$D(E_z) = \exp\left[-2\int_{s_1}^{s_2} dz\{2m_z[U(z)-E_z]/\hbar^2\}^{1/2}\right],$$

where the integration variable z is the position normal to the tunneling barrier, m_z is the effective mass of the tunneling carriers in the direction normal to the barrier, $U(z)$ is the tunneling barrier potential, and s_1 and s_2 are the points where the carrier's longitudinal kinetic energy E_z is just equal to $U(z)$ at the edges of the barrier. The calculation of the barrier penetration probability assumes a trapezoidal tunneling barrier with height Φ_1 relative to the Fermi surface on the superconducting side of the barrier, height Φ_2 on the tip side, width s, and area A. The barrier parameters are chosen to fit experimental conductance-voltage characteristics outside the gap region using a least-squares deviation fitting routine.

For the superconducting density-of-states function I use a modified BCS-like density of states[16]

$$\rho(E,\hat{\mathbf{k}}) = |E-E_f|/[(E-E_f)^2 - \Delta^2(E,\hat{\mathbf{k}})]^{1/2},$$

where $\Delta(E,\hat{\mathbf{k}}) = \Delta_{ab}\sin^2\Theta + \Delta_c\cos^2\Theta$, and $\cos\Theta = \hat{\mathbf{k}}\cdot\hat{\mathbf{c}}$. This functional form for the dependence of the gap on angle is that given by Bennett[17] in the limit of weak anisotropy and assuming a BCS-like interaction potential. Previous treatments of the effects of gap anisotropy on the observed I-V characteristics of high-T_c tunnel junctions[16,18,19] have not taken into account the effects of low-tunneling barrier heights and large energy gaps, nor have they considered the particular anisotropic gap function described here, which I have chosen to be consistent with both the point-contact tunneling results and those from other experimental techniques. Anisotropy in the effective mass of the superconductor is handled by assuming that the effective mass is isotropic in the a-b plane: $m_a = m_b = m_{ab}$. An effective Hamiltonian is written with effective masses in the tunneling frame of reference: $m_x = m_{ab}$, $m_y^{-1} = \cos^2\theta/m_{ab} + \sin^2\theta/m_c$, and $m_z^{-1} = \sin^2\theta/m_{ab} + \cos^2\theta/m_c$, where $\cos(\theta) = \hat{\mathbf{c}}\cdot\hat{\mathbf{z}}$. In doing this I implicitly ignore a cross term in the transformed Hamiltonian which is identically zero if $\theta = 0°$, if $\theta = 90°$, if $m_c = m_{ab}$, or if $k_y = 0$. The numerical results presented below in Fig. 2 are therefore only qualitatively correct for intermediate angles, but are exact (within the limits of the model) for $\theta = 0°$ and $\theta = 90°$.

The solid line in Fig. 1 is an experimental curve for tunneling into a ceramic sample of $La_{2-x}Sr_xCuO_4$ with a Pt point-contact tip.[9] The dashed curves are numerical integrations of Eq. (1) with the model outlined above. In this figure, $\theta = 0°$ corresponds to tunneling primarily along the c-axis direction, and $\theta = 90°$ corresponds to tunneling primarily parallel to the a-b plane. For these curves $T_c = 36$ K, $2\Delta_c = 2kT_c$, and $2\Delta_{ab} = 6.2kT_c$. The best-fit barrier parameters are $\Phi_1 = 23$ meV, $\Phi_2 = 7$ meV, $s = 21$ Å, and $A = 1100$ Å^2, and the Fermi energy of the

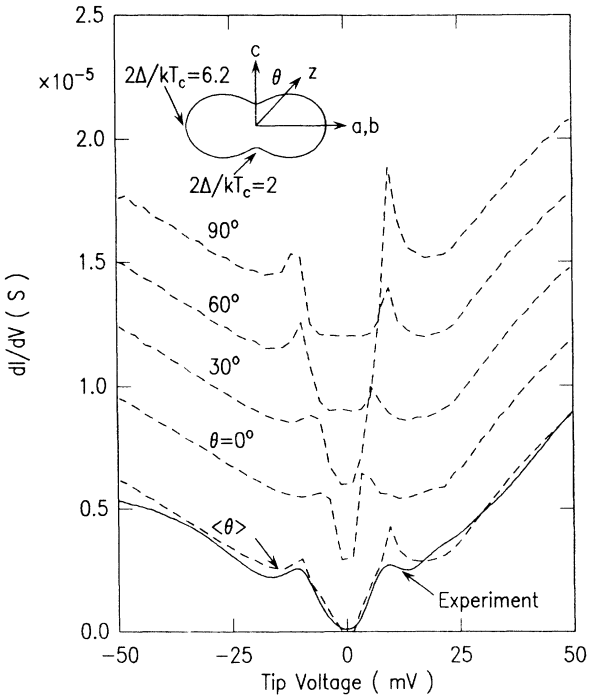

FIG. 1. The solid line is experimental data for tunneling into a ceramic sample of $La_{2-x}Sr_xCuO_4$ (Ref. 9). The dashed curves are numerical integrations of Eq. (1) for an assumed anisotropic gap function (inset), for various angles between the crystalline c-axis direction, and the tunneling junction normal direction (z). The noise in the dashed curves is artificial, resulting from a triple numerical integration over sharply peaked density-of-states functions.

superconductor is taken to be 0.2 eV.[18] The point-contact measurements are made with the tunneling tip indenting the sample. It is therefore not unreasonable for very low-tunneling barrier heights to result.

To approximate the experimental geometry, in which the tip indents the sample, the lower-dashed curve in Fig. 1 represents a simple average over θ of the theoretical curves. The theoretical curves have sharper structure at the gap edges than experiment, but the general form of the experimental curves are reproduced: (i) The linear dependence of the background conductance on voltage, and the asymmetry of this background conductance, are well reproduced by the barrier parameters chosen. (ii) The smearing of the gap edges, which results in this modeling from averaging over different gap values from different crystalline orientations, as well as different tunneling wave vectors from the same crystalline orientation, is also well reproduced by the theory. (iii) The asymmetry in the height of the conductance overshoot at the gap edges is predominantly due to the tunneling carriers having a higher effective barrier height for one bias direction than for the other because of the comparable size of the energy gap to the tunneling barrier. This results in a larger structure at positive tip bias (as observed) if the tunneling carriers are holes (or $q = e$), even for a symmetric barrier. In the modeling leading to Fig. 1 the effective masses in the superconductor were taken to be

isotropic, with $m_c = m_{ab} = m$.

A similar comparison of this model with experiment for $YBa_2Cu_3O_7$ is shown in Fig. 2. Here the solid line is the result for point-contact tunneling into a single crystal of $YBa_2Cu_3O_7$ from a Pt tip,[20] with the tip approach made in the c-axis direction. The experimental curve shows a decided double-humped structure that has been reproduced in many other tunneling measurements of $YBa_2Cu_3O_7$.[21-23] The dotted line in Fig. 2 is a fit to the data of Eq. (1), using a Gaussian distribution of gaps model[24] with two Gaussian distributions with $\Delta_1 = 16$ meV, $\Delta_2 = 30$ meV, and a distribution width for each of $\delta\Delta = 5$ meV, with barrier parameters $E_f = 0.2$ eV, $q = e$, $\Phi_1 = 65$ meV, $\Phi_2 = 19$ meV, and $s = 22$ Å. The good agreement between this model and experiment suggests that the double-humped structure seen in tunneling into $YBa_2Cu_3O_7$ is due to two characteristic gap energies. The dashed curves in Fig. 2 are the result of a full integration of Eq. (1), using the same barrier parameters as for the dotted curve, and taking values for the anisotropic gap function consistent with the infrared results of Collins *et al.*,[1] with $2\Delta_{ab} = 8kT_c$, and $2\Delta_c = 3.53kT_c$, with T_c taken to be 90 K. The effective masses were taken as $m_{ab} = m_e$ and $m_c = 20m_e$, to display the effects of mass anisotropy. Figure 2 makes it arguable that the two gap energies result from a sum of the contributions from carriers tunneling parallel and perpendicular to the large gap axis of an anisotropic superconductor. The high-voltage peaks in the angle-averaged curve come from tunneling parallel to the a-b plane, the lower-voltage shoulders come from tunneling into the c-axis direction. Although the onset of conduction for this assumed density of states occurs at a voltage corresponding to $2\Delta = 3.53kT_c$ the conductance shoulder from this tunneling channel appears at significantly higher voltages because of the averaging in of higher gap values. A comparison of Figs. 1 and 2 shows that one effect of mass anisotropy is to allow significant mixing of the c-axis gap into the tunneling characteristic even when the nominal tunneling direction is parallel to the a-b plane. This happens because the Fermi surface has little dispersion in the c-axis direction, so that tunneling at large angles relative to this axis is allowed. However, once an angular average is done, the results are qualitatively similar independent of the degree of mass anisotropy assumed. The simple linear averaging of the chosen anisotropic gap function in Fig. 2 tends to underestimate the c-axis contribution and overestimate the a-b plane contribution to the experimentally observed total tunneling current. Hall measurements of $YBa_2Cu_3O_7$ (Ref. 25) indicate hole carriers in the a-b plane, and electron carriers in the c-axis direction. The data shown in Fig. 2 are fit much better by the choice $q = e$ (holes) than $q = -e$. This implies that the Fermi level of the superconductor was aligned closer to the valence band than the conduction band of the insulating gap in the tunneling barrier.

Although the numerical modeling used here is an improvement over previous work, it is still oversimplified. The theoretical curves in Figs. 1 and 2 result from the assumption of a very simple gap function, valid in the limit of small anisotropy. The superconducting Fermi surface is taken to be closed, and in a single band, whereas it is likely that the actual Fermi surfaces are nearly two-dimensional and may involve more than one band.[26] Nevertheless, important qualitative conclusions can be drawn from this modeling. First, anisotropy in the gap is predicted to show up quite clearly in the tunneling spectrum if sufficiently smooth and abrupt tunneling geometries can be achieved experimentally. Second, the assumption of gap anisotropy provides a natural explanation for the double-peaked structure observed in tunneling into $YBa_2Cu_3O_7$, and for the smearing of the gap structures always observed in tunneling into the high-T_c superconductors. Most importantly, this model naturally reconciles the results from several different gap-measurement techniques.

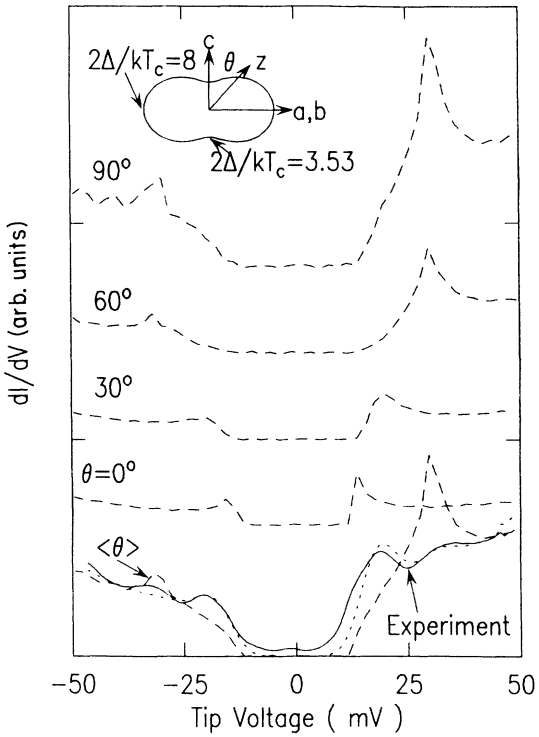

FIG. 2. The solid line is experimental data for tunneling into a single crystal of $YBa_2Cu_3O_7$, from a Pt tip which approached the sample along the c-axis direction (Ref. 20). The dotted curve is a fit of a two-gap model to the data. The dashed curves are numerical integrations of Eq. (1) for an assumed anisotropic gap function (inset), for various angles between the crystalline c-axis direction and the tunneling junction normal direction (z).

I would like to thank R. T. Collins and Z. Schlesinger for many long and patient discussions, and for encouraging me to compare the predictions of an anisotropic gap model with the tunneling results, and T. Penney and D. Newns for educating me on the implications of the sign of the tunneling carriers.

[1]R. T. Collins *et al.*, Phys. Rev. Lett. **63**, 422 (1989); Z. Schlesinger *et al.*, Phys. Rev. B (to be published).
[2]S. L. Cooper *et al.*, Phys. Rev. B **37**, 5920 (1988); S. L. Cooper *et al.*, *ibid.* **38**, 11934 (1988).
[3]Akio Yamanaka *et al.*, Jpn. J. Appl. Phys. **27**, L1902 (1988).
[4]J. M. Imer *et al.*, Phys. Rev. Lett. **62**, 336 (1989).
[5]J. E. Demuth *et al.*, Phys. Rev. Lett. **64**, 603 (1990).
[6]J. C. Phillips, *Physics of High-T_c Superconductors* (Academic, New York, 1989), pp. 238–250.
[7]J. R. Kirtley, Int. J. Mod. Phys. B (to be published).
[8]J. S. Tsai *et al.*, Physica C **153–155**, 1835 (1988).
[9]J. R. Kirtley *et al.*, Phys. Rev. B **35**, 7216 (1987).
[10]K. Flensberg *et al.*, Phys. Rev. B **38**, 841 (1988).
[11]C. Varma, Phys. Rev. Lett. **63**, 1996 (1990).
[12]John Kirtley *et al.*, Phys. Rev. B **14**, 3177 (1976).
[13]R. T. Collins *et al.*, Appl. Phys. Lett. **44**, 533 (1984).
[14]C. B. Duke, *Tunneling in Solids* (Academic, New York, 1969), p. 53.
[15]G. I. Rochlin, Phys. Rev. **153**, 513 (1967).
[16]S. Maekawa *et al.*, in *Novel Superconductivity,* edited by S. A. Wolf and V. Z. Kresin (Plenum, New York, 1987), p. 411.
[17]A. J. Bennett, Phys. Rev. **104**, A1902 (1965).
[18]T. Schneider *et al.*, Z. Phys. B **76**, 3 (1989).
[19]G. D. Mahan, Phys. Rev. B **40**, 2200 (1989).
[20]J. R. Kirtley *et al.*, Phys. Rev. B **35**, 8846 (1987).
[21]J. Geerk *et al.*, Z. Phys. B **73**, 329 (1988).
[22]A. Fournel *et al.*, Europhys. Lett. **6**, 653 (1988).
[23]M. Gurvitch *et al.*, Phys. Rev. Lett. **63**, 1008 (1989).
[24]J. R. Kirtley *et al.*, J. Vac. Sci. Technol. A **6**, 259 (1988).
[25]T. Penney *et al.*, Phys. Rev. B **38**, 2918 (1988).
[26]F. Herman *et al.*, Phys. Rev. B **36**, 6904 (1987).